

Key Results from Physics Studies at DIII-D and TEXTOR in Support of RMP ELM Control at ITER

O. Schmitz¹, T.E. Evans², M.E. Fenstermacher³, B.D. Bray², N.H. Brooks², J.W. Coenen¹, H. Frerichs¹, M.W. Jakubowski⁵, R. Laengner¹, C.J. Lasnier³, A.W. Leonard², R.A. Moyer⁶, S. Mordijck⁶, T.H. Osborne², H. Reimerdes⁷, D. Reiter¹, U. Samm¹, M.J. Schaffer², H. Stoschus¹, B. Unterberg¹, E.A. Unterberg⁴ and the DIII-D and TEXTOR Teams

¹ Forschungszentrum Jülich GmbH, Institut für Energieforschung - Plasmaphysik, Association EURATOM-FZJ, Trilateral Euregio Cluster, 52425 Juelich, Germany

² General Atomics, P.O. Box 85608, San Diego, California 92186-5608, USA

³ Lawrence Livermore National Laboratory, Livermore, California 94550, USA

⁴ Oak Ridge National Laboratory, Oak Ridge, Tennessee, USA

⁵ Max Planck Institute for Plasma Physics, Association EURATOM-MPI, 17491 Greifswald, Germany

⁶ University of California, San Diego, La Jolla, California 92093-0417, USA

⁷ Columbia University, New York, New York, USA

e-mail contact of main author: o.schmitz@fz-juelich.de

Abstract. In this paper key results of a comparison of TEXTOR and DIII-D experiments with external resonant magnetic perturbation (RMP) fields are presented. These comparisons of resistive L-mode plasmas at TEXTOR to highly conductive H-mode plasmas at DIII-D identify generic physics mechanisms of the application of RMP fields with a strong field line pitch angle alignment in the plasma edge. We show evidence that a stochastic edge layer in both very different plasma regimes is induced with at least a thin layer of open field lines in the plasma edge breaking the axis-symmetry of the tokamak introducing a new three-dimensional plasma boundary. In both plasma regimes a reduction of the electron pressure p_e with increasing extension of the vacuum modeled stochastic layer and p_e recovery with decreasing layer width is found caused by a q_{95} resonant reduction of the electron temperature $T_e(q_{95})$. The potential to reduce the RMP induced particle pump out by fine tuning of the RMP spectral properties is shown. At low resonant field amplitudes enhanced particle confinement is found in high field side limited L-mode discharges on both devices while higher resonant field amplitude yield particle pump out.

1. Introduction

The operation of high temperature plasmas in the high confinement mode (H-mode) [1] needed for fusion energy production results in new challenges to be solved for next step fusion experiments. One task crucial to the success of ITER, is the control of edge instabilities inherent to H-mode plasmas, the edge localized modes (ELMs). They endanger the wall integrity of ITER, shorten the life time of plasma facing components and reduce the plasma performance [2]. Large, type-I ELMs were completely suppressed at the DIII-D [3] tokamak by small edge resonant magnetic perturbation (RMP) fields [4, 5]. As this technique is the only one which successfully demonstrated the potential to control type-I ELMs, RMP coils similar to those at DIII-D are designed for ITER. To prepare this undertaking, application of RMP fields is also explored at JET [6], MAST [7] and NSTX [8] and preparations are being made to equip practically every large divertor tokamak in the world with in-vessel RMP coils [9]. For understanding of the physics basis of this promising technique, comparison of experimental observations during RMP application at different devices with a range of plasma shapes and operational regimes are useful. In this paper we compare results of the TEXTOR [10] tokamak with circular, high field side

(HFS) limited L-mode plasmas to both, HFS-limited L-mode and lower single-null divertor H-mode plasmas with RMP ELM suppression at DIII-D. These comparing revealed surprising commonalities which motivated new analysis paths on specific aspects of RMP ELM control. We survey three key aspects investigated in this comparative approach. In Sec. 2, the formation of a three-dimensional (3D) plasma boundary is shown on the example of the measured divertor target heat and particle fluxes and correlated modeling with the EMC3-Eirene plasma and neutral transport Monte-Carlo code [11, 12] adapted to poloidal divertor geometry [13, 14]. In Sec. 3, a potential physical mechanism for the q_{95} resonant nature of ELM suppression by RMP is suggested based on comparison to L-mode plasmas at TEXTOR. In Sec. 4, the control of the particle confinement by fine tuning of the RMP spectral amplitudes as demonstrated at TEXTOR [15, 16] is compared to accompanying experiments at DIII-D showing the potential to maintain high density during RMP ELM control by fine tuning the RMP spectral properties. The consequences of these results for RMP ELM control at ITER are discussed in Sec. 5.

2. Three-Dimensional Plasma Surface Fluxes

The first question during RMP application to a high temperature, rotating, magnetized plasma is how far the external fields penetrate into the plasma and what magnetic topology is formed. As no theory available captures all aspects of plasma transport and the magnetic equilibrium on a sufficient level to yield a self-consistent description of the problem, experimental results documenting features which can be related to the magnetic topology are essential to guide the development of self-consistent models in future. The most direct approach is the inspection of heat and particle fluxes onto the plasma facing components, in particular the divertor target surfaces. At TEXTOR the external RMP field is applied with the *Dynamic Ergodic Divertor (DED)* [17], a set of 16 in-vessel coils mounted at the high field side aligned to the field line pitch angle at HFS on the $q = 3$ surface. RMP field spectra with three dominant poloidal (m) and toroidal (n) mode numbers can be applied, i.e. $m/n = 3/1, 6/2, 12/4$. At DIII-D, the external RMP field is applied as a combination of the in-vessel I-coils [5] and the ex-vessel C-coils used for error field correction. The spectrum is more complex and contains broader harmonics in the $n = 1$ and $n = 2$ sidebands. However, the main $n = 3$ field is as well pitch aligned to $q = 3$. As a result of the pitch alignment of both RMP spectra, comparable three-dimensional particle and heat fluxes patterns are observed on both devices.

Figure 1 shows an example from TEXTOR. The left side of the figure shows the helical particle flux pattern in $m/n = 12/4$ base mode as modeled with the EMC3-Eirene code for TEXTOR [18] compared to the measured D_α distribution on the DED target [19].

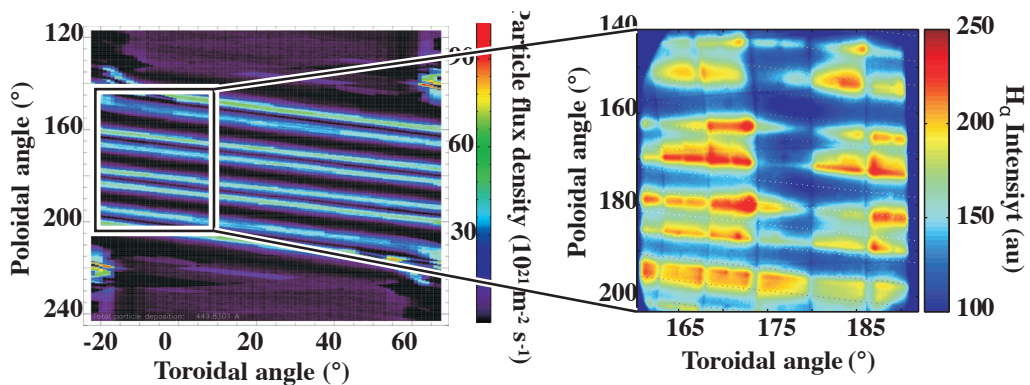


FIG. 1. Particle flux in the RMP induced 3D plasma boundary at TEXTOR. Comparison of the EMC3-Eirene result (left figure) with the measured H_α distribution (right side).

The model shows that the incoming heat and particle fluxes are determined by the local magnetic field line topology [19, 20]. Stochastic field lines with a long connection length travel on chaotic paths through the perturbed edge layer penetrating (in vacuum approximation) as deep as 20% of the minor radius into the plasma and carry the peak heat and particle flux densities. At the very edge of the perturbed layer, field lines with short connection length are bundled into correlated flux tubes forming a helical scrape-off-layer (SOL). The area wetted by those laminar field lines covers about 90% of the magnetic target footprint and therefore the absolute particle and heat flux arriving at the target along stochastic and laminar fields lines is similar [19].

The comparison between the vacuum modeled magnetic footprint and the measured heat flux was used to validate the vacuum approach for TEXTOR conditions employing a generic concept of perturbed Hamiltonian systems: the invariant manifolds of the field line trajectories on the resonant surfaces [21, 22]. These manifolds represent the envelope of the field line trajectories and therefore define the direct connection from one given radial point in the perturbed edge to the wall. Identifying the imprint of the manifolds in the divertor heat flux is therefore a direct proof of stochastisation of the rational surface connected by this manifold. In Refs. [20] and [22], a one to one correlation between the vacuum modeled manifold connections and the heat flux imprint was revealed for a range of edge safety factor values. This suggests the validity of the vacuum approach for modeling of the perturbed topology for TEXTOR L-mode plasmas at high resonant field amplitudes $B_r \sim 0.1B_p$, with B_p being the poloidal magnetic field. Under these conditions with high resistivity and low rotation a dissipation of screening currents and a topology similar to the vacuum case was also expected from recent drift fluid modeling [23]. Imaging of magnetic islands in the plasma edge [21] and plasma profile properties [24] in agreement with vacuum field lines tracing at Tore Supra support this finding for L-mode plasmas in circular limiter geometry. However, at lower perturbation strength and higher rotation a screening of the RMP field is expected and was found in experiment rotating the DED imposed RMP field [25]. In combination this shows that for high resonant field amplitudes, a vacuum like topology is found defining target flux patterns as well as electron density and temperature fields in the 3D boundary [19].

During ELM suppression by RMP at DIII-D a similar decomposition of the rational flux surfaces as observed at TEXTOR was expected along with a decomposition of the divertor separatrix into stable and unstable manifolds [21]. This results in a 3D striated divertor heat and particle flux pattern which was observed consistently in ELM suppressed H-modes in low averaged triangularity $\bar{\delta} \sim 0.3$ with high electron pedestal collisionality $\nu_e^* \sim 2$ [26] and in ITER similar shape, high $\bar{\delta} \sim 0.55$ and low $\nu_e^* \sim 0.1$ plasmas. An example is presented in Fig. 2 showing the D_α emission in the lower divertor in (a) a rectangular view from the top down into the divertor for the inner strike point (ISP), (b) the outer strike point (OSP) and (c) in a tangential view. This striation observed during RMP ELM suppression is typically accompanied by an enhanced negative floating potential at the divertor surface [27] and an increase of the heat flux at the target

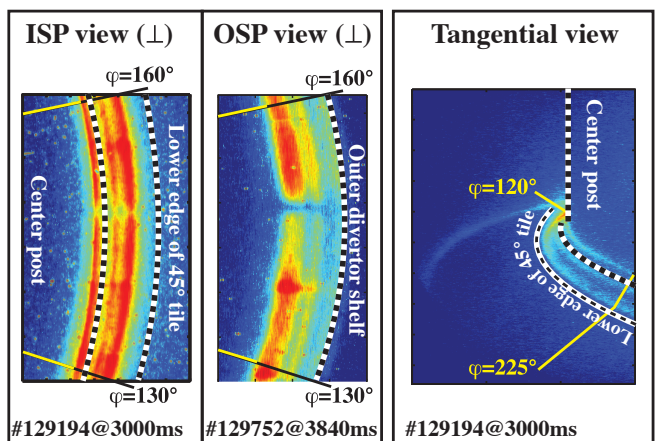


FIG. 2. Particle flux striation during RMP ELM suppression at DIII-D: from left to right: inner strike point, outer strike point, tangential view.

surface compared to the inter ELM heat flux [28], both indicating that open field lines from inside the separatrix reach the divertor surface. Moreover, the narrow striation of the D_α and also CII emission observed can only be explained by a strong variation of the plasma parameters along the target due to predominant parallel transport along the open field lines [14]. These reliable observations provide substantial evidence, that during RMP ELM suppression a 3D plasma boundary with least a thin layer of open, perturbed field lines exists [29]. This was recently supported by a similar analysis at NSTX [30].

3. Resonant Feature of Edge Transport and ELM Control

Another robust feature of complete ELM suppression is the strong dependence on the safety factor q_{95} at the $\Psi_N = 95\%$ flux surface in normalized toroidal flux Ψ_N [5, 31].

Figure 3 shows a survey for plasmas at low triangularity $\bar{\delta} \sim 0.3$ (green markers) compared to high triangularity $\bar{\delta} \sim 0.55$ (blue markers). The width of the q_{95} window is depicted as a function of (a) the sum of the $q = m/n = 3$ resonant amplitudes $\sum B_r^{m,n}$ at $q = 3$ with $(m/n = 3/1, 6/2, 9/3, 12/4)$ (left side of figure) and (b) the width $\Delta\tilde{\Psi}_N$ of the open perturbed layer (right side).

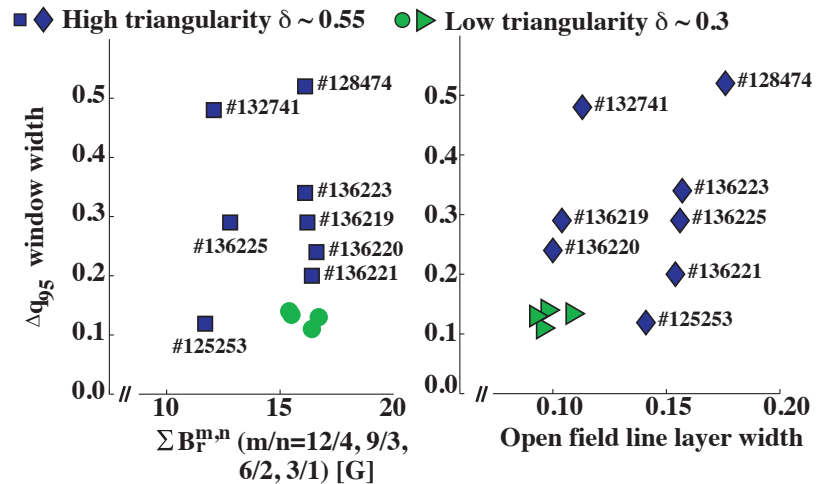


FIG. 3. Resonant RMP ELM suppression windows in low averaged triangularity ($\bar{\delta} \sim 0.3$) and in high $\bar{\delta} = 0.55$.

This quantity was calculated by tracing a set of $> 20,000$ field lines on lengths scales of the electron mean free path at $\Psi_N = 0.95$ evaluating the deepest radial point in Ψ_N reached on this length scale. This connects the idea of a ballistic transport along the mean free path with the field line dynamics. This analysis shows that for low $\bar{\delta}$ plasmas a typical window width $\Delta q_{95} = 0.1 - 0.15$ for full suppression exists at $\sum B_r^{m,n} \sim 17$ G and $\Delta\tilde{\Psi}_N \sim 0.1$. For high $\bar{\delta}$ plasmas the width Δq_{95} for full suppression is as in nearly all cases wider than for low $\bar{\delta}$ and offers attractive operational points. For ITER, the requirement is a wide window Δq_{95} at minimal resonant field amplitudes and small perturbed layer width. Discharge #132741 for example is an attractive candidate for this operational point. However, as Fig. 3 shows, a wide variation of Δq_{95} and the resonant amplitudes and perturbed layer width needed is found. There is no clear correlation of Δq_{95} with either the $\sum B_r^{m,n}$ nor the $\Delta\tilde{\Psi}_N$ in the set of discharges analyzed and more detailed understanding of the physical mechanisms determining the ELM suppressed window is required. One attempt was made in comparing the electron pressure profile $p_e(\Psi_N, q_{95})$ response to a systematic scan in q_{95} . The safety factor q_{95} was scanned in these experiments matching a resonant ridge of the external RMP spectrum applied to maximize the resonant components [32]. The result is depicted in Fig. 4 with $p_e(\Psi_N, q_{95})$ for DIII-D in Figs. 4(a,c) and $p_e(\Psi_N, q_a)$ for TEXTOR in Figs. 4(b,d).

For DIII-D a clear modulation in $p_e(\Psi_N, q_{95})$ is seen with the strongest decrease inside of the q_{95} resonant window with ELM suppression. This supports the hypothesis that the peeling ballooning type ELMs are stabilized due to a flattening of the pressure gradient ∇p_e in the plasma edge (e.g. [5]). A comparable experiment in a very different plasma regime, i.e. circular shape, high field side limited L-mode plasma at TEXTOR reproduced

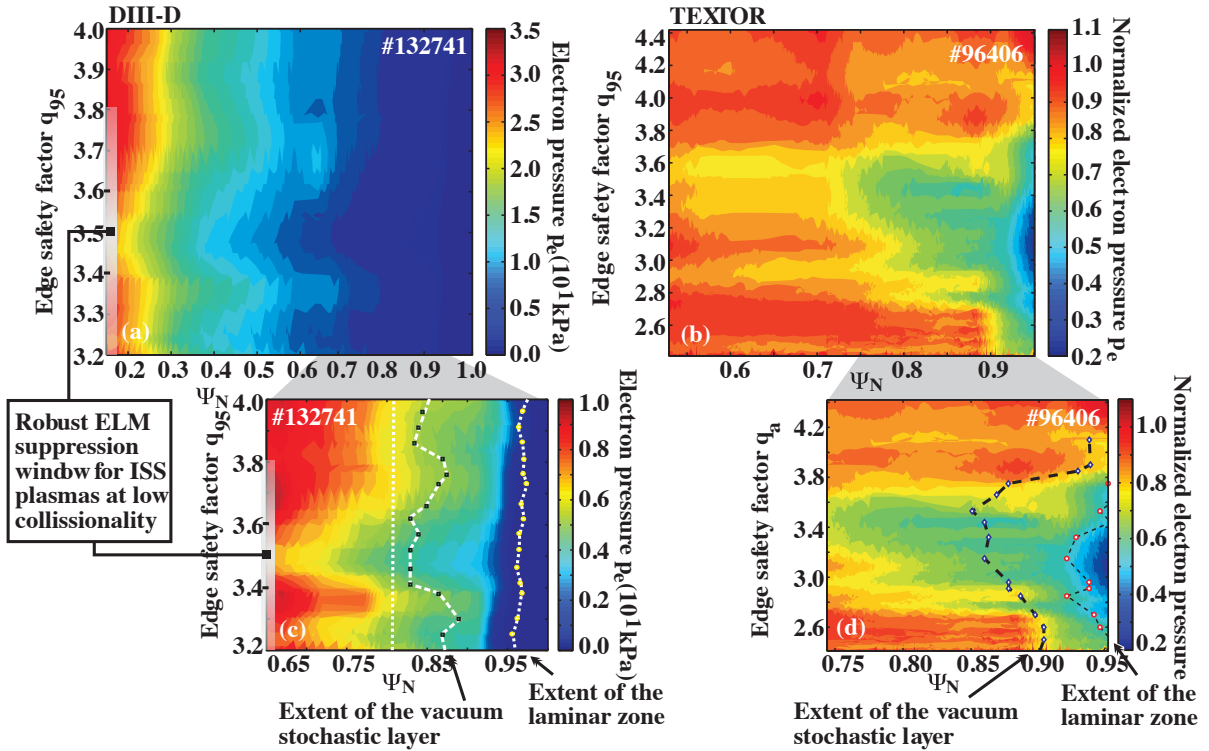


FIG. 4. Pressure $p_e(\Psi_N, q_{95})$ during application of a comparable, field line pitch angle aligned edge resonant RMP field at DIII-D (a,c) and TEXTOR (b,d).

this result as shown in Figs. 4(b,d). The electron pressure is strongly decreased in a resonant window in $q_a = 3.0 - 3.6$ and the whole pressure profile is affected, not only the edge. This q_{95} dependent modulation of p_e is caused on both devices by a overall decrease of the electron density n_e (density pump out) and a highly q_{95} dependent modulation of the electron temperature T_e [32]. This modulation in T_e is found to be correlated on both experiments to the extension of the stochastic layer width while the very edge is determined by the laminar flux tubes as a new, 3D SOL. This is depicted in Fig. 4(c) for DIII-D and Fig. 4(d) for TEXTOR. The stochastic and laminar zone width is overlaid to the edge $p_e(q, \Psi_N)$ field. For increasing extension of the stochastic layer, a stronger decrease in p_e is observed with a p_e recovery for decreasing layer width. As the p_e modulation is induced by the underlying T_e sensitivity to the safety factor and the related stochastic layer width, this finding from both devices supports enhanced thermal transport as potential reason for the q_{95} resonant ELM suppression at DIII-D. However, the actual p_e value is not directly linked to the ELM suppressed windows [32] as the actual profile shape determines if the plasma is peeling-ballooning (P-B) stabilized or not. Therefore the causality between stochastic layer induced T_e reduction causing a p_e decrease stabilizing the P-B type modes is indirect only. In addition, the actual topology in the edge depends on the accuracy of the plasma equilibrium. Edge bootstrap currents for instance can not yet be measured at DIII-D but they are an important ingredient to model the stochastic layer width [33].

The decrease of both $n_e(\Psi_N)$ and $T_e(\Psi_N)$ is not restricted to the plasma edge but both profiles are reduced in the pedestal as well as in the core, as shown in Fig. 5(a,b) in a comparison of ELM averaged profiles before RMP application (green profiles) and a profile averaged across the whole ELM suppressed window (red profile). In contrast the ion temperature $T_i(\Psi_N)$ is reduced at the pedestal but steepens in mid radius and increases in the plasma center by 20%. At the same radial position an increase in the rotational shear is measured which indicates the formation of an ion transport barrier at mid radius connected to ELM suppression.

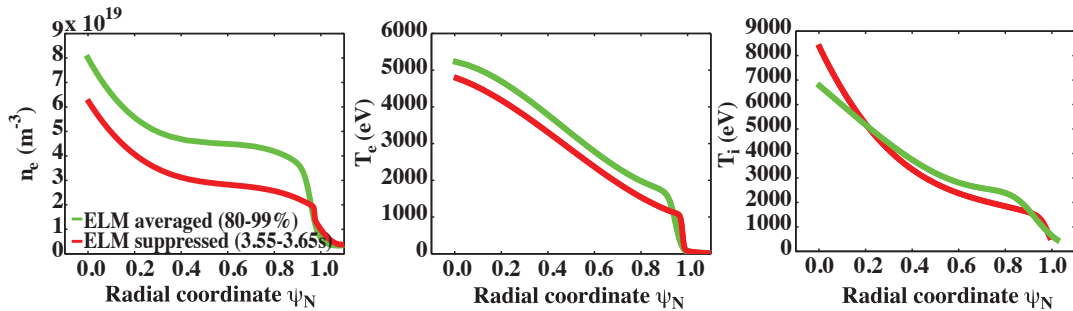


FIG. 5. Plasma electron density, temperature and ion temperature profiles during ELMs (green profiles) and for RMP ELM suppressed H-mode (red profiles) at DIII-D).

4. Particle Confinement Control by RMP

As discussed in the section before, one inherent feature of ELM suppression and also of ELM control on other devices [6, 7, 8] is the so-called density pump out, i.e. a reduction of the plasma density and the plasma confined total number of particle N_{tot} . However, at ITER the plasma density has to be maintained to match the fusion gain of $Q=10$. Therefore methods to avoid the density pump out are required to optimize the ELM suppression by RMP fields for ITER. At TEXT and Tore Supra it was shown that by shifting the plasma position the density in a plasma under RMP application can be either enhanced or reduced [21]. At TEXTOR it was demonstrated that for fixed plasma position, enhanced particle confinement can be achieved by fine tuning of the resonant amplitudes and the location of the resonant flux surface [15]. Subsequently it was shown, that just by manipulating the resonant amplitudes a transition between enhanced particle confinement and particle pump out can be realized [16]. This TEXTOR result is exemplarily shown in Fig. 6(a,c) depicting the electron density profiles $n_e(Z)$ across the plasma column.

In the first case [Fig. 6(a)] a small DED current amplitude of $I_{DED} = 1.5$ kA yields an increase of the entire $n_e(Z)$ profile. As the particle confinement is dependent on both the fueling and of the transport mechanisms it is strongly affected by the plasma source. This plasma source is transformed into a 3D shape as discussed in Sec. 2 and might also undergo changes concerning the overall intensity and the resulting fueling mechanisms.

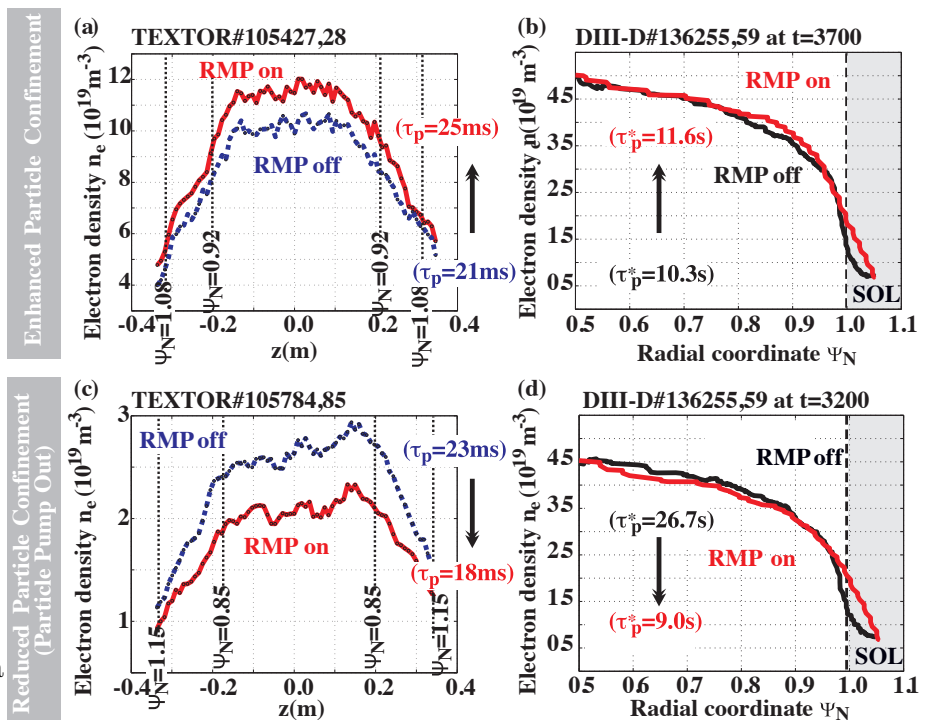


FIG. 6. Particle confinement control by RMP fields shown with electron density profiles for TEXTOR (left column, figs (a) and (c)) and DIII-D (right column, figs (b) and (d)).

Therefore a particle balance is needed to really judge the changes in the particle content with RMP fields applied. For this purpose a comparable single reservoir particle balance model was applied for TEXTOR and DIII-D [16, 34]. This balance shows for the case under discussion, the 20% increase of $n_e(Z)$ is a result of an equivalent increase in the particle confinement time τ_p of $\Delta\tau_p = 4ms$, i.e. 20%. Raising the DED current amplitude to $I_{DED} = 7.5kA$, the typical particle pump out with a 30% reduction of $n_e(Z)$ and 20% reduction in τ_p is found. The transition between both particle confinement regimes was inspected in more detail by DED current scans as reported in [16] and it was shown that the enhanced particle confinement improves gradually with increasing (small) resonant amplitudes and a marginal opening of the outermost dominant resonant island chain. This increase is in direct correlation to an enhanced radial electrical field shear Ω_{ExB} which vanishes when the laminar zone touches the resonant surface transforming the enhanced particle confinement into particle pump out.

The same transition was achieved in experiments with slightly elongated, high field side limited L-mode plasmas at DIII-D. The current in the I-coil was kept constant and the resonant amplitude on a given rational flux surfaces was scanned by small variations of the edge safety factor q_{95} . Figure 6(b) shows the $n_e(\Psi_N)$ profile for a case with a low resonant amplitude of $\sum B_r^{m,n} = 7.2G$ at the $q = 3$ surface. The density profiles steepens in the plasmas edge and a small increase at the top of the density shoulder ($\Psi_n \sim 0.88$) is seen. However, the s_{wall} term, i.e. the measure for the wall recycling flux increases for this RMP setup which results in a 10% increase in the effective particle confinement time τ_p^* (see [34] for the particle balance applied). Reducing q_{95} increases $\sum B_r^{m,n} = 9.9G$ at the $q = 3$ surface and yields particle pump out with a reduction in the $n_e(\Psi_N)$ towards the plasma center and an increase in the SOL with a reduction in τ_p^* by a factor of 2.6.

5. Discussion and Conclusion

The results surveyed in this paper show comparable experimental observations in experiments with RMP fields applied to high field side limited L-mode at TEXTOR and DIII-D and diverted H-mode discharges at DIII-D. The formation of a 3D plasma boundary with at least a thin layer of open field lines was revealed comparing the redistributed divertor particle and heat fluxes on both devices. The plasma surface fluxes are controlled by the vacuum modeled perturbed magnetic footprint which suggests that this is a feasible method for the analysis of the plasma wall interaction with RMP ELM control at ITER. As the 3D flux redistribution itself and the potential changes in the quantitative fluxes are likely to change the resulting gross- and net-erosion [35], this finding is important for the analysis of the consequence of a potential ELM control coil set for ITER.

For ITER similar shape H-mode plasmas at high triangularity and at low ν_e^* with ELM suppression at DIII-D and high field side limited L-mode plasmas at TEXTOR, an enhancement of the electron thermal transport was found depending on the stochastic layer extent. This analysis of the electron pressure resonance in connection to ELM suppression and the investigation of the underlying energy and particle transport changes indicates that for high $\bar{\delta}$ plasmas in ISS shape at low ν_e^* , an overall reduction of n_e with a highly q_{95} sensitive enhancement of the electron thermal transport seems to be a prerequisite of the q_{95} resonant feature of ELM suppression while an improvement in the ion energy confinement maintains the overall confinement and probably the plasma in H-mode at all. Recently an even more sensitive dependence of the frequency of mitigated ELMs on q_{95} at JET was reported [36]. This finding was not compatible with a resonance in the stochastic layer width but interpreted by a modification of the peeling part of the peeling-ballooning type-I ELMs. However, such cross-machine comparison is hampered by the differences in the RMP coil sets and the resulting RMP spectra and the deviating

experimental observations therefore point out the importance to account for the generic differences like RMP spectrum, coil geometry etc.. The advantage of the DIII-D and TEXTOR comparison presented here is the similarity of the RMP spectrum in terms of a good field line pitch angle alignment in the plasma edge.

An improved particle confinement was found for high field side limited L-mode plasmas and low resonant field amplitudes reproducing basic results from TEXTOR at DIII-D. Increasing the RMP amplitudes yield particle pump out with a reduction of the enhanced radial electric field shear measured possibly due to an increase in the vacuum modeled stochastic layer width. These results show a path for maintaining high density at ITER under ELM control by RMP by fine tuning the RMP spectral amplitudes. However, this mechanism has to be reproduced in a high triangularity plasma where the high magnetic shear compresses the resonant flux surface and might make the fine tuning of the local resonant field impact more difficult.

This work was supported by the US Department of Energy under DE-FG03-97ER54415, DE-AC52-07NA27344, DE-FC02-04ER57698, DE-FG02-07ER54917, DE-FG02-05ER54809, DE-AC05-OOR22725 and DE-FG02-89ER53297.

References

- [1] WAGNER, F., et al., Phys. Rev. Lett. **49** (1982) 1408
- [2] LOARTE, A., et al., Plasma Phys. Control. Fusion **45** (2003) 1594
- [3] LUXON, J.L., et al., Nucl. Fusion **42** (2002) 614
- [4] EVANS, T.E., et al., Phys. Rev. Lett. **92** (2006) 235003-1
- [5] EVANS, T.E., et al., Nature Phys. **2** (2006) 419
- [6] LIANG, Y., et al., Nucl. Fusion **50** (2010) 025013
- [7] NARDON, E., et al., Plasma Phys. Control. Fusion **51** (2009) 124010
- [8] CANIK, J.M., et al., Nucl. Fusion **50** (2010) 034012
- [9] FENSTERMACHER, M.E., et al., this conference, ITR/P1-30
- [10] NEUBAUER, O., et al., Fusion Sci. Technol. **47** (2005) 46
- [11] FENG, Y., et al., J. Nucl. Mater. **241-243** (1997) 930
- [12] REITER, D., et al., Fusion Sci. Technol. **47** (2005) 172
- [13] FRERICHS, H., et al., Computational Phys. Comm. **181** (2010) 61-70
- [14] FRERICHS, H., et al., Nucl. Fusion **50** (2010) 034004
- [15] FINKEN, K.H., et al., Phys. Rev. Lett. **98** (2007) 065001
- [16] SCHMITZ, O., et al., J. Nucl. Mater. **390-391** (2009) 299
- [17] FINKEN, K.H., et al., Nucl. Fusion **39** (1999) 637
- [18] KOBAYASHI, M., et al., Nucl. Fusion **44** (2004) S64-S73
- [19] SCHMITZ, O., et al., Nucl. Fusion **48** (2008) 024009
- [20] JAKUBOWSKI, M.W., et al., J. Nucl. Mater. **373-365** (2007) 671
- [21] EVANS, T.E., *“Chaos, Complexity and Transport,”* World Scientific, Singapore, 2008
- [22] WINGEN, A., et al., Phys. Plasmas **14** (2007) 042502
- [23] REISER, D., et al., Phys. Plasmas **16** (2009) 042317
- [24] GHENDRIH, Ph., et al., Nucl. Fusion **42** (2002) 1211
- [25] STOSCHUS, H., et al., Phys. Plasmas **17** (2009) 1
- [26] EVANS, T.E., et al., J. Phys. Conf. Series **7** (2005) 174
- [27] WATKINS, J.G., et al., J. Nucl. Mater. **363-365** (2007)
- [28] JAKUBOWSKI, M.W., et al., Nucl. Fusion **49** (2009) 095013
- [29] SCHMITZ, O., et al., Plasma Phys. Control. Fusion **50** (2008) 124029
- [30] AHN, J.W., et al., Nucl. Fusion **50** (2010) 045010
- [31] FENSTERMACHER, M.E., et al., Phys. Plasmas **15** (2008) 056122
- [32] SCHMITZ, O., et al., Phys. Rev. Lett. **103** (2009) 165005
- [33] HUDSON, B., et al., Nucl. Fusion **50** (2010) 045006
- [34] UNTERBERG, E.A., et al., Nucl. Fusion **49** (2009) 092001
- [35] SCHMITZ, O., et al., “The Influence of Three-Dimensional Stochastic Boundaries on Plasma Edge Transport and the Resulting Plasma-Wall Interaction,” accepted for publication in J. Nucl. Mater. (2010)
- [36] LIANG, Y., et al., Phys. Rev. Lett. **105** (2010) 065001